IEEE Access
Multidisciplinary | Rapid Review | Open Access Journal

Received September 23, 2018, accepted October 14, 2018, date of publication October 18, 2018,
date of current version November 14, 2018.

Digital Object Identifier 10.1109/ACCESS.2018.2876760

Bandwidth-Enhanced Cavity-Backed Magneto-Electric Dipole Antenna

LEI CHANG[1,2], JIAN-QIANG ZHANG[1,2], LING-LU CHEN[1], AND BAO-MING LI[1]
[1]No. 36 Research Institute of CETC, Jiaxing 314033, China
[2]Academician Workstation, Zhejiang Longyou Gongren Electronics Co., Ltd., Quzhou 324014, China

Corresponding author: Lei Chang (yutian_1986@163.com)

This work was supported by the Young Elite Scientists Sponsorship Program by CAST under Grant 2017QNRC001.

ABSTRACT A cavity-backed directional magneto-electric dipole antenna with enhanced impedance and gain bandwidths is presented, which is excited by a coaxial balun. The proposed antenna contains a rectangular parasitic element, a modified metal cavity, as well as a bowtie dipole with bending structures. The enhanced impedance and gain bandwidths are achieved by using the rectangular parasitic element and modified cavity. Two pairs of vertical metal plates with different heights and a horizontal metal plate are applied in the modified cavity. In the low-working frequency band, the combination of the bowtie dipole, the horizontal metal plate, and a pair of vertical metal plates with lower height acts as a magnetic dipole, as well as the rectangular parasitic element located above the bowtie dipole functions as a director. A new magnetic dipole is excited by combining the rectangular parasitic element and the bending structures in the high-working frequency band. The experimental results show that the antenna has an impedance bandwidth of 1.38–3.55 GHz (88%) for $S_{11} \leq -15$ dB. In addition, low cross-polarization, high front-to-back ratio, stable radiation patterns, and a boresight gain of 9.05 ± 1.01 dBi are obtained in the whole operating band.

INDEX TERMS Magneto-electric dipole, cavity-backed antenna, bandwidth enhancement, gain.

I. INTRODUCTION

Modern radar and communication systems develop rapidly and have great demand for higher performance antennas, such as wider bandwidth, better impedance matching, higher gain, and stable radiation patterns. Therefore, many studies have been carried on to implement these properties. Metasurface has been used for enhancing the gain of antennas [1], [2]. To obtain good impedance matching with $S_{11} \leq -15$ dB, some non-unidirectional antennas have been presented with fractional bandwidths of 8.7% [3], 31% [4], and 66.7% [5], respectively. However, they cannot be used in the point-to-point communication systems. Several unidirectional antennas, such as ridged horn and log-periodic dipole antennas, are not suitable for some space limited communication systems.

To achieve wideband unidirectional radiation patterns and compact size, dipole and bowtie antennas with reflectors are studied. In [6], a wideband dipole antenna with corrugated-reflectors is proposed. The impedance bandwidth for VSWR ≤ 2 is 100.9%, and the gain is greater than 6 dBi in the band of 2.75-6 GHz (74.3%). An impedance bandwidth for $S_{11} \leq -10$ dB and bandwidth for gain $\geq$ 8.2 dBi of a dipole antenna are 113% (1.15-4.07 GHz) and 96.6% (1.15-3.3 GHz), respectively [7]. But the maximum radiation direction of the antenna on xoz-plane is not at $\theta = 0°$ of 2.55-3.3 GHz band. A cavity-backed dipole antenna fed by a microstrip coupling line obtains a 117% impedance bandwidth for VSWR ≤ 2 and a 108.9% bandwidth for gain ≥ 6 dBi [8]. A nonplanar dipole antenna is proposed in [9], which has a 112.5% impedance bandwidth for VSWR ≤ 2 and stable unidirectional radiation patterns at 2.8-6 GHz (72.7%). In [10], an opened loop is applied to a unidirectional dipole antenna to improve the impedance bandwidth. The antenna has an impedance bandwidth of 101.7% (VSWR ≤ 2). A cavity-backed bowtie antenna achieves a 91.4% impedance bandwidth for VSWR ≤ 2 [11]. A circular ring is applied to obtain stable unidirectional radiation patterns. In [12], a unidirectional folded bowtie antenna with a cavity structure obtains a 92.2% impedance bandwidth for $S_{11} \leq -10$ dB. A unidirectional antenna composed of a folded sectorial bowtie and a composite cavity structure is presented to obtain an impedance bandwidth of 143% for VSWR ≤ 2 [13]. In [14], a cavity-backed bowtie antenna loaded with parasitic stubs achieves a 117% bandwidth for VSWR ≤ 2 and unidirectional radiation patterns.

Wideband unidirectional dipole antennas with better impedance matching are also studied [15]–[17]. An impedance bandwidth of 59.7% for VSWR $\leq$ 1.5 and stable gain are obtained by using four dipoles and a reflector of a dipole antenna [15]. The height of the antenna is $0.499\lambda_L$ (λ_L is the free-space wavelength at the starting frequency). In [16], by using a folded dipole and an L-shaped coupling fed structure, a broadband base station antenna obtains an impedance bandwidth of 53% for $S_{11} \leq -15$ dB. A unidirectional full-wavelength dipole antenna using a hybrid feeding structure has an impedance bandwidth of 32% for $S_{11} \leq -14$ dB [17].

Wideband unidirectional antennas realized by magneto-electric (ME) dipole have led to a growing interest. By introducing a shorted bowtie structure, wideband ME dipoles are obtained with impedance bandwidths of 60% [18] and 87% [19] for VSWR ≤ 2, respectively. In [20] and [21], a horizontal folded bowtie electric dipole is used, and impedance bandwidths of 95.2% and 110% for VSWR ≤ 2 are achieved, respectively. A differential-fed method is used, and a 114% impedance bandwidth for VSWR ≤ 2 is achieved [22]. Two U-shaped bowtie elements as an electric dipole and a horned reflector with two layers are applied to a ME dipole [23], which can improve impedance matching and radiation patterns, respectively. This antenna achieves a 118% impedance bandwidth for VSWR $\leq$ 2. A multilayer printed circuit board method is applied to a ME dipole antenna [24]. By adopting this method, an impedance bandwidth of 110% for VSWR $\leq$ 2 is achieved. Wideband unidirectional ME dipole antennas are also studied to achieve better impedance matching [25]–[27]. A ME dipole with a U-shaped reflector is proposed [25], which achieves a 51.5% impedance bandwidth for VSWR $\leq$ 1.5. ME dipoles with a planar reflector [26] and with a metal cavity structure [27] achieve impedance bandwidths of 45.6% and 54.8% respectively for VSWR $\leq$ 1.5.

In this paper, a wideband ME dipole antenna by introducing a rectangular parasitic element and a modified metal cavity is studied for achieving enhanced impedance and gain bandwidths. The simulated current distributions of the proposed antenna are discussed. In the low operating band, the direction of the current on the rectangular parasitic element is the same as that of the current on the bowtie electric dipole. The parasitic element functions as a director. A magnetic dipole is generated by combining the modified metal cavity and the bowtie dipole. In the high operating band, the rectangular parasitic element and the bending structures act as a new magnetic dipole. We present a modified metal cavity which has two pairs of vertical plates with different heights, as well as analyze the effects of the cavity on the impedance matching and gain. Furthermore, the results of experiment and simulation are provided and discussed.

II. ANTENNA DESIGN

The proposed ME dipole with dimensions of 148 mm $\times$ 113 mm $\times$ 44 mm is composed of a rectangular parasitic element, a modified metal cavity, a bowtie dipole, and a coaxial feed structure. The thickness of all metal plates is 0.5 mm. The geometry of the proposed cavity-backed ME dipole antenna is depicted in Fig. 1.

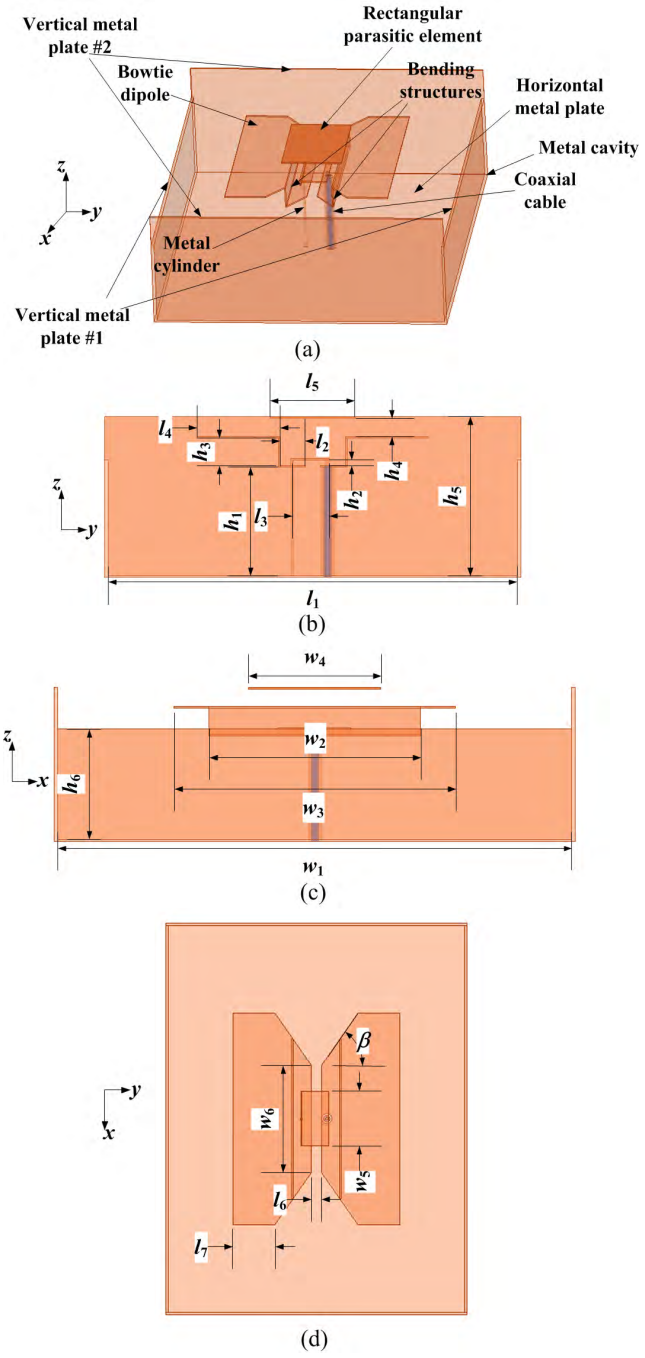

FIGURE 1. Geometry of the proposed cavity-backed ME dipole antenna: (a) 3D view; (b) side view 1; (c) side view 2; (d) bowtie dipole.

As shown in Fig. 1, the bowtie dipole comprises bending structures with a gap of l_6 and a height of h_3, as well as a pair of traditional patches. The patch contains a rectangular part (with dimensions of $l_7 \times w_3$) and a trapezoid part. The lengths of two parallel sides of trapezoid part are w_2 and w_3 respectively. A rectangular parasitic element with dimensions

TABLE 1. Dimensions of proposed cavity-backed ME dipole antenna.

Parameters	Values	Parameters	Values
l_1	113 mm 0.52 $_L$	l_2	7 mm 0.032 $_L$
l_3	10.1 mm 0.046 $_L$	l_4	23 mm 0.106 $_L$
l_5	23.5 mm 0.108	l_6	4 mm 0.018 $_L$
l_7	16 mm 0.074 $_L$	w_1	148 mm 0.681 $_L$
w_2	60.99 mm 0.281 $_L$	w_3	80.99 mm 0.373 $_L$
w_4	38 mm 0.175 $_L$	w_5	21 mm 0.097 $_L$
w_6	41 mm 0.189 $_L$	h_1	30 mm 0.138 $_L$
h_2	1.4 mm 0.006 $_L$	h_3	7.5 mm 0.035 $_L$
h_4	5 mm 0.023 $_L$	h_5	44 mm 0.202 $_L$
h_6	32 mm 0.147 $_L$		55°

$_L$ is the free-space wavelength at the starting frequency at 1.38 GHz.

of $l_5 \times w_4$ is placed h_3 above the bowtie dipole. A modified metal cavity is introduced to improve the operating bandwidth of the antenna, which contains a horizontal metal plate and two pairs of vertical metal plates with different heights. The dimensions of the horizontal metal plate are $l_1 \times w_1$. The heights of two pairs of vertical metal plates are h_5 and h_6, respectively. The distance between the bending structures and the horizontal metal plate is h_1. A coaxial balun is used to feed the antenna. A bowtie arm and horizontal metal plate are connected by the conducting outer metal tube of coaxial line. The other bowtie arm and the central conducting core of the coaxial line are connected by an inverted L-shaped metal structure with dimensions of $l_3 \times w_5 \times h_2$ instead of a folded central conducting core used in [28]. A metal cylinder with diameter of 1 mm is used to connect this arm and the horizontal metal plate.

Detailed dimensions of the proposed antenna are shown in Table 1.

λ_L is the free-space wavelength at the starting frequency at 1.38 GHz.

III. ANTENNA OPERATION PRINCIPLE

Fig. 2 shows the simulated current distributions of the antenna at 1.4, 2.6 and 3.2 GHz. We can see from Fig. 2(a) that the directions of the current on the rectangular parasitic element and the bowtie electric dipole are the same. The parasitic element acts as a director. Similar to [29], as the director is used, the impedance bandwidth can be improved. The combination of the horizontal metal plate, the vertical metal plate #1, and the bowtie dipole works as a magnetic dipole. The magnetic dipole plays an important role on reducing the low cutoff frequency. Fig. 3(a) shows the simulated electric

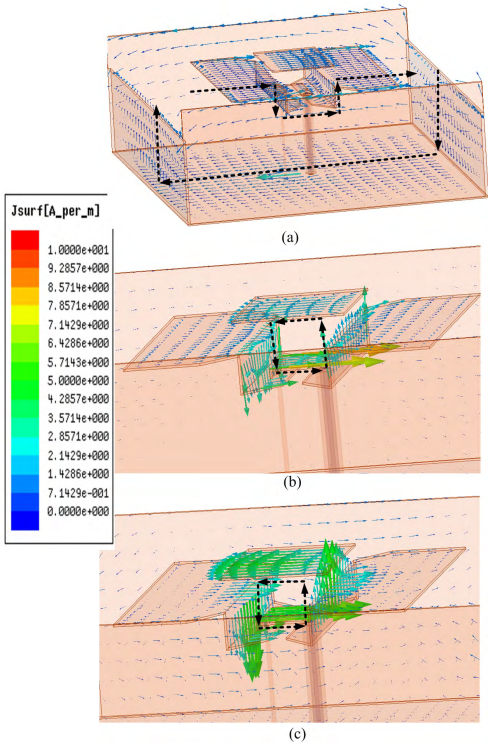

FIGURE 2. Current distributions of the antenna at (a) 1.4, (b) 2.6 and (c) 3.2 GHz.

fields at 1.4GHz. It can be seen that the electric fields are distributed along y-axis and a magnetic dipole along x-axis is realized. As shown in Fig. 2(b) and Fig. 3(b), a new magnetic dipole is generated by the combination of the bending structures and the parasitic element. In Fig. 2(c), the magnetic dipole plays a main role and the radiation of the bowtie electric dipole is decreased.

A. EFFECT OF THE MODIFIED METAL CAVITY

Fig. 4 shows comparisons of simulated S_{11} and boresight gain of the proposed antenna with and without metal cavity (two pairs of vertical metal plates are removed). It can be seen that the low cutoff frequency of the antenna for $S_{11} \leq -15$ dB is moved from 1.657 GHz to 1.389 GHz and the impedance matching over the whole band is improved when the two pairs of vertical metal plate are added. The simulated impedance bandwidth for $S_{11} \leq -15$ dB is from 1.389 to 3.557 GHz. The boresight gain of the antenna without vertical metal plates decreases significantly near 3.2 GHz. Comparisons of simulated radiation patterns with and without metal cavity at 1.7 and 3.5 GHz are shown in Fig. 5. When the metal cavity is introduced, the front-to-back ratio is significantly increased and the beamwidth of the H-plane narrows in the high-frequency band.

We study the effects of vertical metal plate #1 and vertical metal plate #2 on the antenna performance, respectively. Simulated S_{11} and boresight gain of the proposed antenna without vertical metal plate #1 (with vertical metal plate #2)

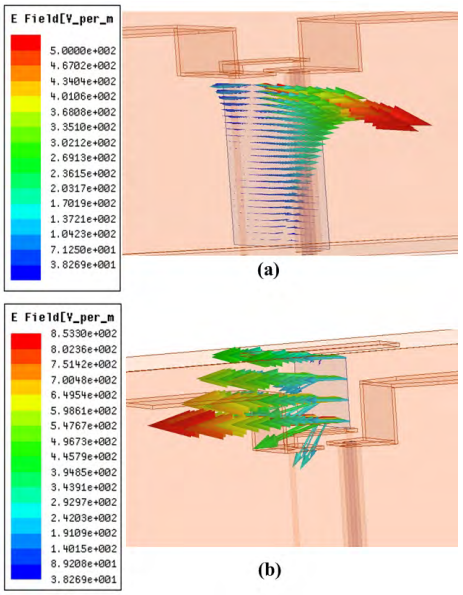

FIGURE 3. Simulated electric fields of the antenna at (a) 1.4 and (b) 2.6 GHz.

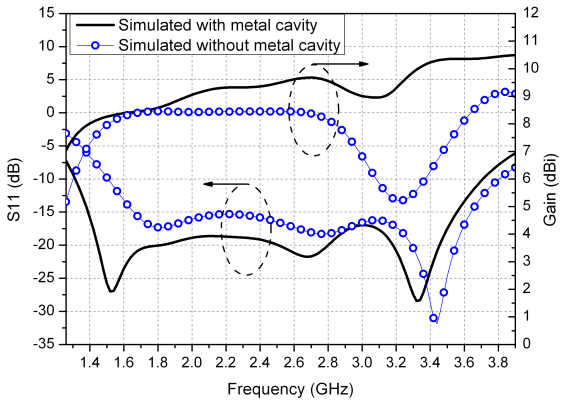

FIGURE 4. Comparisons of simulated S_{11} and boresight gain with and without metal cavity.

are shown in Fig. 6(a). It can be seen that when vertical metal plate #1 is removed, the impedance matching in the band of 1.389-2.8 GHz deteriorate and the boresight gain is decreased in the band of 1.389-1.6 GHz. Fig. 6(b) shows the simulated S_{11} and boresight gain of the proposed antenna without vertical metal plate #2, while vertical metal plate #1 is added. It is shown that vertical metal plate #2 has a significant effect on the gain over the whole operating band. When vertical metal plate #2 is applied, a better impedance matching is achieved in the bands of 1.389-1.6 GHz and 2.8-3.4 GHz. Figs. 7 and 8 show the impacts of vertical metal plate #1 and #2 on the radiation patterns, respectively. Vertical metal plate #1 has significant influence on the front-to-back ratio in the high-frequency band, while vertical metal plate #2 mainly affects the front-to-back ratio in the low-frequency band. Moreover, vertical metal plate #2 is the main reason for the narrow beamwidth of the H-plane in the high-frequency band.

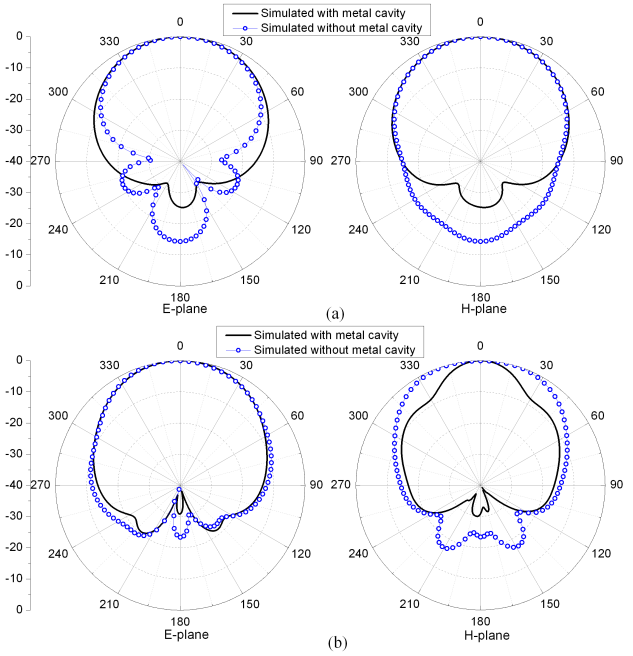

FIGURE 5. Comparisons of simulated radiation patterns with and without metal cavity at (a) 1.7 GHz and (b) 3.5 GHz.

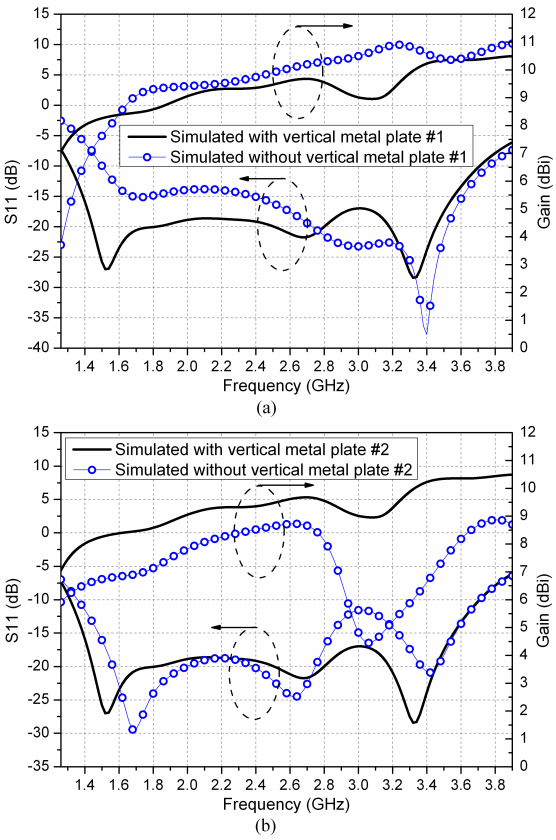

FIGURE 6. Effects of (a) vertical metal plate #1 and (b) vertical metal plate #2.

B. EFFECT OF THE PARASITIC ELEMENT

The rectangular parasitic element is located above the bowtie dipole. The cases with and without parasitic element are

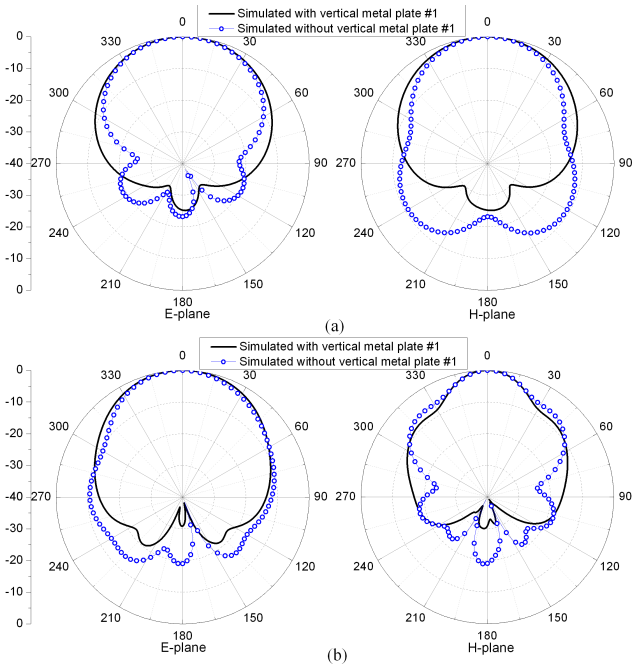

FIGURE 7. Simulated radiation patterns with and without vertical metal plate #1 at (a) 1.7 GHz and (b) 3.5 GHz.

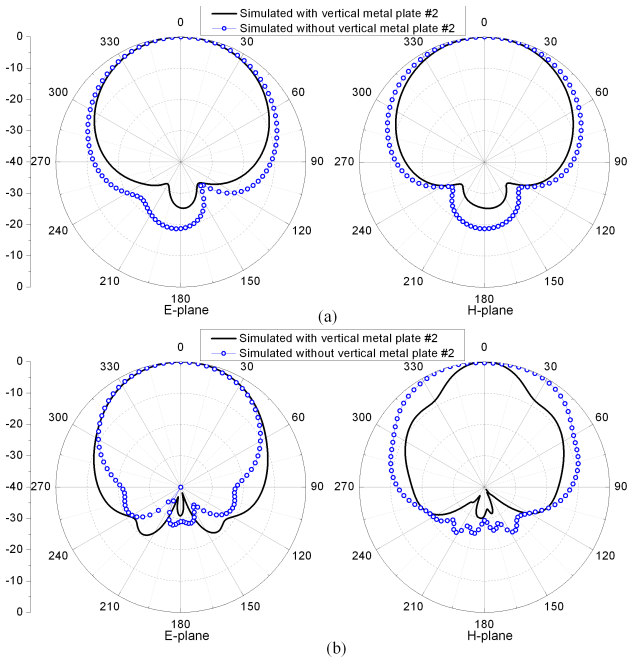

FIGURE 8. Simulated radiation patterns with and without vertical metal plate #2 at (a) 1.7 GHz and (b) 3.5 GHz.

studied (the modified metal cavity is added). The simulated results of S_{11} and boresight gain are shown in Fig. 9. When the parasitic element is removed, the impedance matching becomes worse in the whole band, and the impedance bandwidth for $S_{11} \leq -15$ dB is only from 1.437 to 1.9 GHz, as well as the boresight gain is decreased after 3.2 GHz. Fig. 10 shows the effects of the parasitic element on the

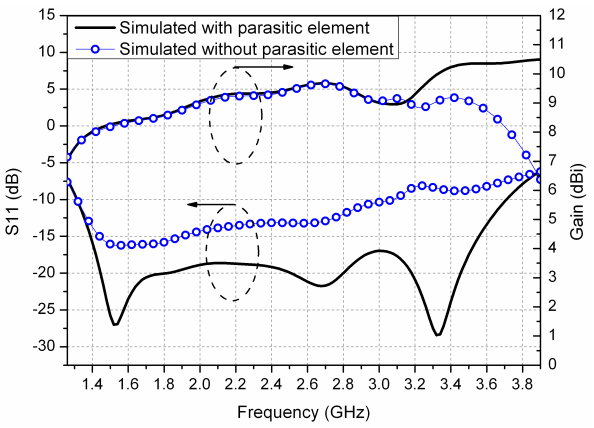

FIGURE 9. Comparisons of simulated S_{11} and boresight gain with and without rectangular parasitic element.

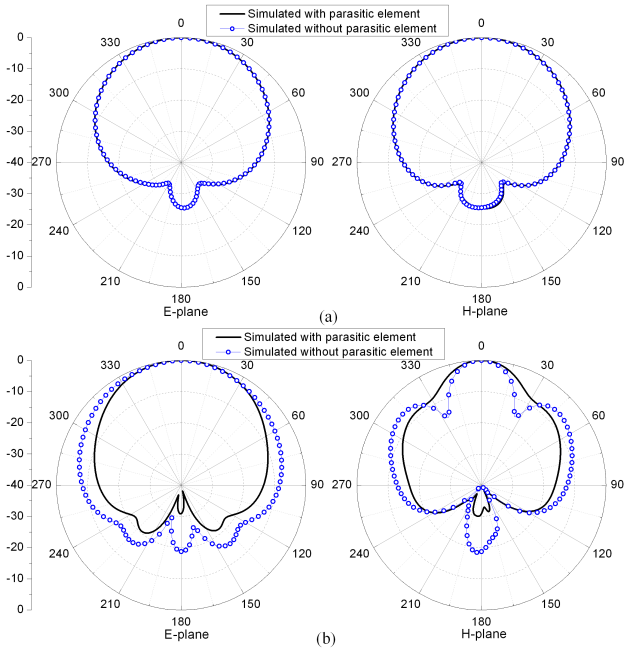

FIGURE 10. Simulated radiation patterns with and without parasitic element at (a) 1.7 GHz and (b) 3.5 GHz.

radiation patterns. The parasitic element has little effect on the radiation patterns in the low-frequency band. However, the radiation patterns of the H-plane are dramatically improved by introducing the parasitic element in the high-frequency band.

C. PARAMETRIC STUDY

We select several important parameters of the parasitic element and modified metal cavity to investigate the effects on the impedance bandwidth.

The influence of the height of vertical metal plate #2 is shown in Fig. 11(a). Compared with $h_5 = 44$ mm, the impedance matching performance gets worse a little with $h_5 = 41$ mm near 3.0 GHz; while with $h_5 = 47$ mm, the results of S_{11} are increased a little from 2.1 to 2.5 GHz.

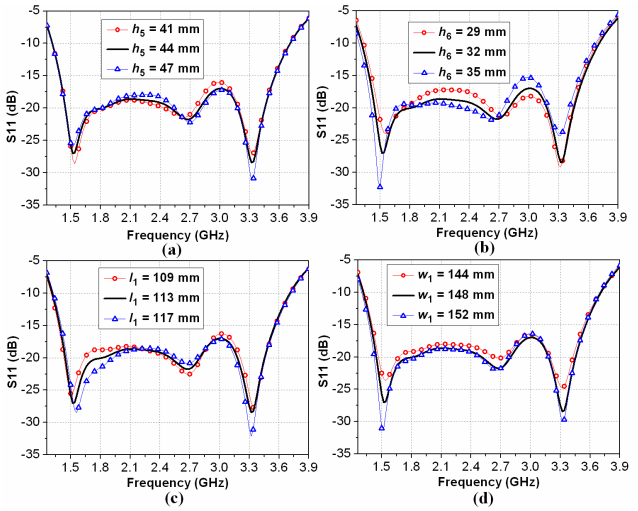

FIGURE 11. Simulated S_{11} with different values of (a) h_5, (b) h_6, (c) l_1, and (d) w_1.

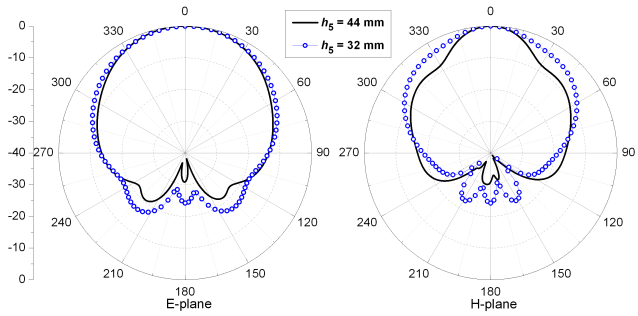

FIGURE 12. Simulated radiation patterns with different values of h_5 at 3.5 GHz.

When h_6 increases, the results of S_{11} are decreased at 1.8-2.7 GHz, but are increased near 3.0 GHz, as shown in Fig. 11(b). The effects of l_1 and w_1 on the S_{11} are shown in Figs. 11(c) and (d). When $l_1 = 109$ mm, the impedance matching performance gets worse near 3.0 GHz. When $w_1 = 144$ mm, the results of S_{11} are increased at 1.4-2.8 GHz. As l_1 and w_1 increase, the change of the impedance matching performance is little. To consider the requirements of compact size, the optimal values of l_1 and w_1 are 113 mm and 148 mm respectively. The effect of h_5 on the radiation patterns is shown in Fig. 12. When h_5 is reduced to 32 mm, symmetric radiation patterns can be obtained in the high-frequency band.

Fig. 13 shows the simulated S_{11} with different values of l_5, w_4, and h_4. It can be seen from Figs. 13(a) and (b) that as l_5 and w_4 decrease, the results of S_{11} near 3 GHz are increased and the third resonant frequency is shifted to the higher frequency; as l_5 and w_4 increase, the third resonant frequency is shifted to the lower frequency and the operating band for $S_{11} \leq -15$ dB narrows. Compared with $h_4 = 5$ mm, the third resonant frequency basically disappears with $h_4 = 3$ mm; while with $h_4 = 7$ mm, the results

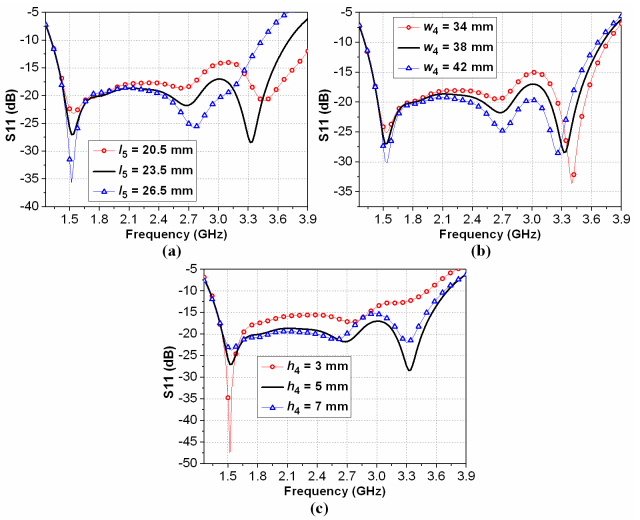

FIGURE 13. Simulated S11 with different values of (a) l_5, (b) w_4, and (c) h_4.

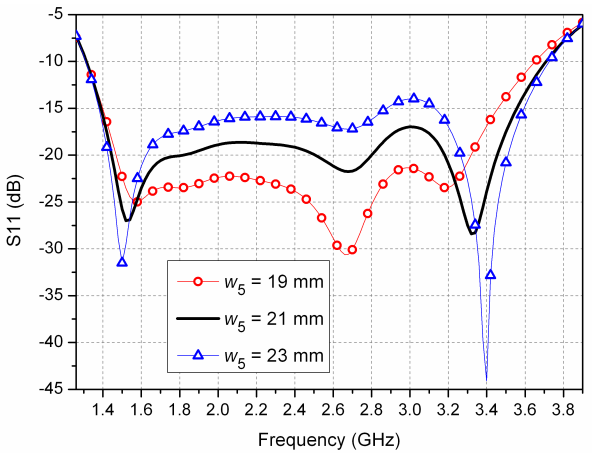

FIGURE 14. Simulated S_{11} with different values of w_5.

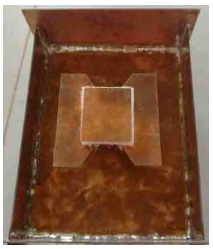

FIGURE 15. Photo of the proposed antenna.

of S_{11} near 3 GHz are increased and the high cutoff frequency is moved to the lower frequency.

As shown in Fig. 14, the impedance matching is influenced noticeably by the width w_5 of inverted L-shaped metal structure. The optimal value of w_5 is determined as 21 mm. As $w_5 = 19$ mm, the high cutoff frequency is shifted to the lower frequency; while $w_5 = 23$ mm, the impedance matching becomes worse in the band of 1.6-3.3 GHz.

TABLE 2. Performance of wideband unidirectional dipole antennas.

	Size $_L = C/f_{Low}$	Impedance matching	BW	Gain (dBi)
[15]	0.62 $_L$×0.62 $_L$× 0.499 $_L$	VSWR ≤ 1.5	59.7% 1.55~2.87 GHz	8.4~9.6
[16]	height: 0.235 $_L$	S_{11} ≤ -15 dB (VSWR ≤ 1.432)	53% 1.65~2.85 GHz	about 9
[17]	1.063 $_L$×0.931 $_L$× 0.224 $_L$	S_{11} ≤ -14 dB (VSWR ≤ 1.5)	32% 698~960 MHz	8.5~8.7
[25]	0.784 $_L$×0.621 $_L$× 0.07 $_L$	VSWR ≤ 1.5	51.5% 1.96~3.32 GHz	5.8~8
[26]	0.806 $_L$×0.806 $_L$× 0.13 $_L$	VSWR ≤ 1.5	45.6% 1.86~2.96 GHz	7.3~8.9
[27]	0.702 $_L$×0.702 $_L$× 0.125 $_L$	VSWR ≤ 1.5	54.8% 1.88~3.3 GHz	7.8~9.4
Prop.	0.681 $_L$×0.52 $_L$× 0.202 $_L$	S_{11} ≤ -15 dB (VSWR ≤ 1.432)	88% 1.38~3.55 GHz	8.04~10.06

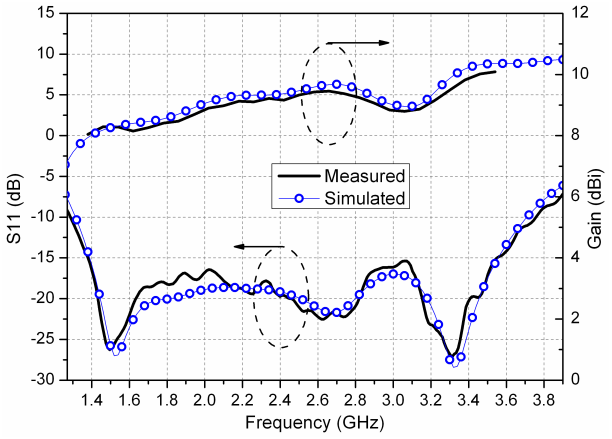

FIGURE 16. Measured and simulated S_{11} of the cavity-backed antenna.

IV. EXPERIMENTAL RESULTS

A prototype of the proposed cavity-backed ME dipole antenna with dimensions shown in Table 1 was fabricated, which is depicted in Fig. 15. The parasitic element was supported by a foam ($\varepsilon_r = 1.05$).

The measured S_{11} and boresight gain are compared with the simulation results, as shown in Fig. 16. The measured impedance bandwidth for $S_{11} \leq -15$ dB is 88% from 1.38 to 3.55 GHz. The measured boresight gain varies between 8.04 and 10.06 dBi.

Comparisons between the recently published dipole antennas and the proposed antenna in term of antenna size, impedance matching, operating frequency band and antenna gain are shown in Table 2. We have found that the proposed antenna shows good impedance matching for $S_{11} \leq -15$ dB, wider impedance bandwidth and higher peak gain. The proposed antenna has a lower height and a smaller area compared to the antennas in [13]–[15]. Antennas in [23]–[25] have a lower height, but have a larger area.

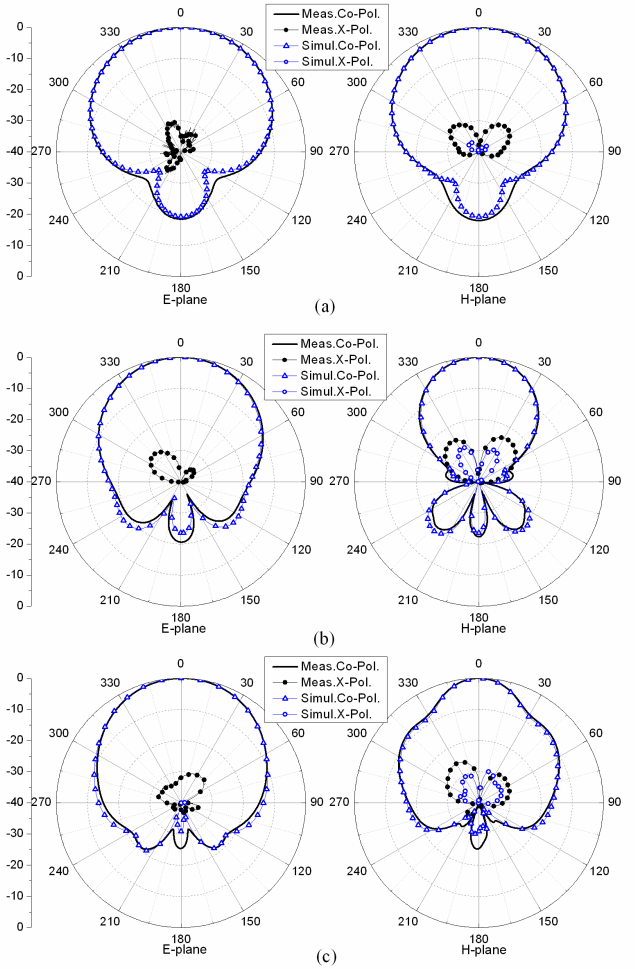

FIGURE 17. Radiation patterns of two principle planes at (a) 1.4 GHz, (b) 2.8 GHz, and (c) 3.5 GHz.

The simulated and measured radiation patterns of the proposed antenna at 1.4, 2.8, and 3.5 GHz are shown in Fig. 17. The stable unidirectional radiation patterns are obtained in the whole operating band. The proposed antenna also achieves low cross polarization and high front-to-back ratio. It can be seen that the measured cross polarization level is less than −20 dB, and the measured front-to-back ratio is greater than 18 dB.

V. CONCLUSION

A wideband magneto-electric dipole antenna is proposed in this paper. The effects of the metal cavity, the parasitic element, and the inverted L-shaped metal structure have been studied. Moreover, the current distributions and electric fields of the proposed antenna are given. Experiments show that the proposed antenna achieves an impedance bandwidth of 88% for $S_{11} \leq -15$ dB, a boresight gain varying between 8.04 and 10.06 dBi, low cross polarization, high front-to-back ratio, and stable unidirectional radiation patterns. The overall size of the proposed antenna is 148 mm × 113 mm × 44 mm. The antenna is a good candidate for many wideband wireless communication systems.

REFERENCES

[1] H.-P. Li, G.-M. Wang, T. Cai, J.-G. Liang, and X.-J. Gao, "Phase- and amplitude-control metasurfaces for antenna main-lobe and sidelobe manipulations," *IEEE Trans. Antennas Propag.*, vol. 66, no. 10, pp. 5121–5129, Oct. 2018, doi: 10.1109/TAP.2018.2858181.

[2] H.-P. Li, G.-M. Wang, X.-J. Gao, J.-G. Liang, and H.-S. Hou, "A novel metasurface for dual-mode and dual-band flat high-gain antenna application," *IEEE Trans. Antennas Propag.*, vol. 66, no. 7, pp. 3706–3711, Jul. 2018.

[3] Y. Wang, A. J. Pretorius, and A. M. Abbosh, "Low-profile antenna with elevated toroid-shaped radiation for on-road reader of RFID-enabled vehicle registration plate," *IEEE Trans. Antennas Propag.*, vol. 64, no. 4, pp. 1520–1525, Apr. 2016.

[4] L. Rufail and J. Laurin, "Aircraft cavity-backed nonprotruding wideband antenna," *IEEE Antennas Wireless Propag. Lett.*, vol. 11, pp. 1108–1111, 2012.

[5] A. Raghunathan, N. U. Shankar, and R. Subrahmanyan, "An octave bandwidth frequency independent dipole antenna," *IEEE Trans. Antennas Propag.*, vol. 61, no. 7, pp. 3411–3419, Jul. 2013.

[6] Q. Wu, R. Jin, J. Geng, and D. Su, "On the performance of printed dipole antenna with novel composite corrugated-reflectors for low-profile ultra-wideband applications," *IEEE Trans. Antennas Propag.*, vol. 58, no. 12, pp. 3839–3846, Dec. 2010.

[7] Z. Wang, J. Wu, Y. Yin, and X. Liu, "A broadband dual-element folded dipole antenna with a reflector," *IEEE Antennas Wireless Propag. Lett.*, vol. 13, pp. 750–753, 2014.

[8] J. Y. Li, R. Xu, X. Zhang, S. G. Zhou, and G. W. Yang, "A wideband high-gain cavity-backed low-profile dipole antenna," *IEEE Trans. Antennas Propag.*, vol. 64, no. 12, pp. 5465–5469, Dec. 2016.

[9] Q. Wu, S. Wang, and X. Sun, "Nonplanar dipole antennas for low-profile ultrawideband applications: Design, modeling, and implementation," *IEEE Antennas Wireless Propag. Lett.*, vol. 11, pp. 897–900, 2012.

[10] Q. Wu, X. Ding, and A. Chen, "A broadband dipole antenna for multi-service indoor distributed antenna system (MS-IDAS)," *IEEE Antennas Wireless Propag. Lett.*, vol. 14, pp. 839–842, 2015.

[11] S. W. Qu, J. L. Li, Q. Xue, and C. H. Chan, "Wideband cavity-backed bowtie antenna with pattern improvement," *IEEE Trans. Antennas Propag.*, vol. 56, no. 12, pp. 3850–3854, Dec. 2008.

[12] S. W. Qu, J. L. Li, Q. Xue, C. H. Chan, and S. M. Li, "Wideband and unidirectional cavity-backed folded triangular bowtie antenna," *IEEE Trans. Antennas Propag.*, vol. 57, no. 4, pp. 1259–1263, Apr. 2009.

[13] S. W. Qu, C. H. Chan, and Q. Xue, "Ultrawideband composite cavity-backed folded sectorial bowtie antenna with stable pattern and high gain," *IEEE Trans. Antennas Propag.*, vol. 57, no. 8, pp. 2478–2483, Aug. 2009.

[14] S.-G. Zhou, G.-L. Huang, and T.-H. Chio, "A low profile, wideband cavity-backed bowtie antenna," *Microw. Opt. Technol. Lett.*, vol. 55, no. 6, pp. 1422–1426, Jun. 2013.

[15] Q. X. Chu and Y. Luo, "A broadband unidirectional multi-dipole antenna with very stable beamwidth," *IEEE Trans. Antennas Propag.*, vol. 61, no. 5, pp. 2847–2852, May 2013.

[16] Y. Cui, R. Li, and P. Wang, "A novel broadband planar antenna for 2G/3G/LTE base stations," *IEEE Trans. Antennas Propag.*, vol. 61, no. 5, pp. 2767–2774, May 2013.

[17] C. Ding, B. Jones, Y. J. Guo, and P.-Y. Qin, "Wideband matching of full-wavelength dipole with reflector for base station," *IEEE Trans. Antennas Propag.*, vol. 65, no. 10, pp. 5571–5576, Oct. 2017.

[18] H. Wong, K. M. Mak, and K. M. Luk, "Wideband shorted bowtie patch antenna with electric dipole," *IEEE Trans. Antennas Propag.*, vol. 56, no. 7, pp. 2098–2101, Jul. 2008.

[19] Z. Y. Zhang, G. Fu, S. X. Gong, and S. L. Zuo, "Wideband unidirectional patch antenna with Γ-shaped strip feed," *Electron. Lett.*, vol. 46, no. 1, pp. 24–26, Jan. 2010.

[20] L. Ge and K. M. Luk, "A wideband magneto-electric dipole antenna," *IEEE Trans. Antennas Propag.*, vol. 60, no. 11, pp. 4987–4991, Nov. 2012.

[21] L. Ge and K. M. Luk, "A magneto-electric dipole for unidirectional UWB communications," *IEEE Trans. Antennas Propag.*, vol. 61, no. 11, pp. 5762–5765, Nov. 2013.

[22] M. Li and K. Luk, "A differential-fed magneto-electric dipole antenna for UWB applications," *IEEE Trans. Antennas Propag.*, vol. 61, no. 1, pp. 92–99, Jan. 2013.

[23] B. Feng, S. Li, W. An, S. Yin, J. Li, and T. Qiu, "U-shaped bow-tie magneto-electric dipole antenna with a modified horned reflector for ultra-wideband applications," *IET Microw., Antennas Propag.*, vol. 8, no. 12, pp. 990–998, Sep. 2014.

[24] K. Kang, Y. Shi, and C.-H. Liang, "Substrate integrated magneto–electric dipole for UWB application," *IEEE Antennas Wireless Propag. Lett.*, vol. 16, pp. 948–951, 2017.

[25] M. J. Li and K. M. Luk, "A low-profile wideband planar antenna," *IEEE Trans. Antennas Propag.*, vol. 61, no. 9, pp. 4411–4418, Sep. 2013.

[26] L. Ge and K. M. Luk, "A magneto-electric dipole antenna with low-profile and simple structure," *IEEE Antennas Wireless Propag. Lett.*, vol. 12, pp. 140–142, 2013.

[27] L. Ge and K.-M. Luk, "A low-profile magneto-electric dipole antenna," *IEEE Trans. Antennas Propag.*, vol. 60, no. 4, pp. 1684–1689, Apr. 2012.

[28] B. Li, Y.-Z. Yin, W. Hu, Y. Ding, and Y. Zhao, "Wideband dual-polarized patch antenna with low cross polarization and high isolation," *IEEE Antennas Wireless Propag. Lett.*, vol. 11, pp. 427–430, 2012.

[29] J. Wu, Z. Zhao, Z. Nie, and Q.-H. Liu, "Design of a wideband planar printed quasi-Yagi antenna using stepped connection structure," *IEEE Trans. Antennas Propag.*, vol. 62, no. 6, pp. 3431–3435, Jun. 2014.

LEI CHANG was born in Tengzhou, Shandong, China, in 1986. He received the B.S. degree in electronic science and technology and the Ph.D. degree in electromagnetic field and microwave technology from Southwest Jiaotong University, Chengdu, China, in 2007 and 2013, respectively. In 2013, he joined the No. 36 Research Institute of CETC, where he is currently a Senior Engineer.

His recent research interests include UWB antenna and millimeter-wave antenna.

JIAN-QIANG ZHANG was born in Longyou, Zhejiang, China, in 1964. He received the B.S. degree in electromagnetic field and microwave technology from the University of Electronic Science and Technology of China, Chengdu, China, in 1985. He is currently a Researcher Grade Senior Engineer with the No. 36 Research Institute of CETC.

His recent research interests include microwave and millimeter-wave antenna, metamaterials, and phase array antenna.

LING-LU CHEN was born in Wuyi, Zhejiang, China, in 1986. She received the B.S. degree in electronic science and technology and the Ph.D. degree in electromagnetic field and microwave technology from Southwest Jiaotong University, Chengdu, China, in 2008 and 2014, respectively. In 2014, she joined the No. 36 Research Institute of CETC, where she is currently a Senior Engineer.

Her recent research interests include UWB antenna and array.

BAO-MING LI was born in Guilin, Guangxi, China, in 1983. He received the B.S. degree in electromagnetic field and microwave technology from the University of Electronic Science and Technology of China, Chengdu, China, in 2006. In 2006, he joined the No. 36 Research Institute of CETC, where he is currently a Senior Engineer.

His recent research interests include reflector antenna and millimeter-wave antenna.